Effects of Turbulence and Lubricant Inertia on Dynamics of Journal Bearings Lubricated with Molten Zinc in a Galvanizing Process

M. Rashidi, A.B. Ebiana, J.T. Sawicki, and R. Sinnadurai

In a galvanizing process a continuous sheet of steel is passed through a bath of molten zinc around a series of rotating rollers. One or more of these rollers are submerged in the bath of molten zinc and are supported by journal bearings that are lubricated with molten zinc. Dynamic characteristics of these bearings influence the quality of the finished galvanized sheet and also determine the production speed. This work presents a theoretical study of these bearings in terms of the damping, stiffness, and inertia coefficients of the film of molten zinc separating the journal from the bearings. This work also addresses the influence of turbulence on the bearing dynamics. The damping, stiffness, and inertia coefficients of journal bearings lubricated with molten zinc are determined for different zinc alloys at 450, 650, and 850 °F.

Keywords
computer analyses, galvanizing, lubricants, turbulence

1. Introduction

IN THE PRODUCTION of galvanized metal sheets, one or two of the guiding rollers are submerged in a molten zinc bath as shown in Fig. 1. The molten zinc acts as the lubricating fluid for the journal bearings supporting the submerged rollers. The dynamic behavior of these bearings, the control of the metal sheet passing through the molten zinc bath, and the vibrational characteristics of the guiding rollers are among the factors that limit the production speed of the galvanizing process. Bearing seizure, lateral vibrations of guide rollers at certain production speeds, and frequent bearing failures are among the problems that have dictated a low rate of galvanizing production. Increases in productivity and quality assurance are obtained via a reasonable understanding of the dynamics of the machinery involved in the manufacturing of the galvanized sheet.

Numerous theoretical and experimental investigations of the design/analysis of journal bearings have been reported in the literature (Ref 1-7). The hydrodynamic lubrication problem has typically been analyzed using the classical Reynolds lubrication theory, which assumes a thin lubricant laminar flow and negligible fluid inertia. However, with the trend toward high-speed bearing design, and the use of low-viscosity, unconventional lubricants such as water or liquid metal, the fluid inertia becomes important and a high Reynolds number can no longer be regarded as negligible. Indeed, the effects of turbulence and inertia of the lubricant film on bearing behavior become more pronounced as the Reynolds number increases. For some range of moderately large Reynolds numbers, classic lubrication models are inadequate to predict bearing performance. An analytical solution can be obtained only with many oversimplifying assumptions and thus gives little insight into the practical problem. Where the problem is not amenable to direct analysis, tedious experimental trial-and-error methods, expensive by nature and confined in results, were considered the only effective means to understand and predict journal bearing behavior oper-

M. Rashidi, A.B. Ebiana, J.T. Sawicki, and **R. Sinnadurai,** Department of Mechanical Engineering, Cleveland State University, Cleveland, Ohio 44115, USA.

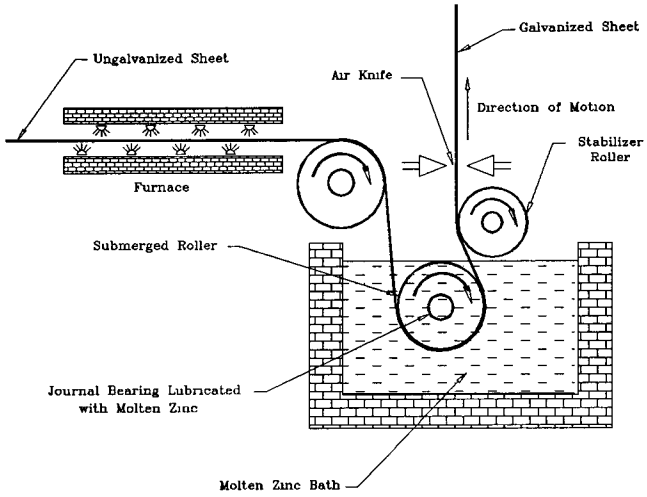

Fig. 1 Schematic view of a galvanizing process

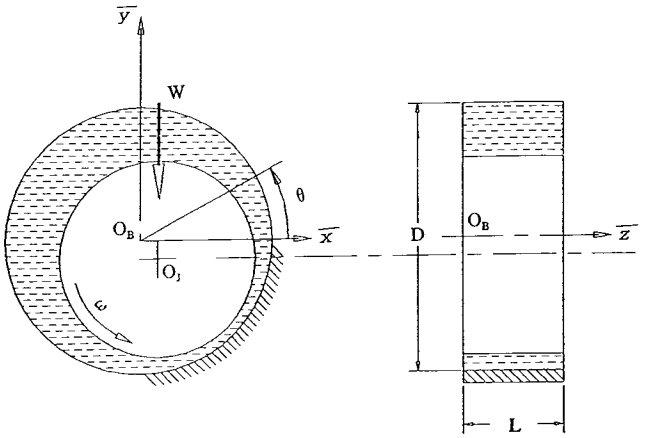

Fig. 2 Notation for the journal bearing. O_B, bearing origin

ating at turbulent regimes. With the advent of digital computers, versatile computational software is now used extensively to overcome the mathematical complexity of the problem.

The present work extends Rashidi's (Ref 8) study of journal bearings lubricated with molten zinc to include the effect of turbulence and inertia of the oil film. The dynamic analysis of the journal bearing was carried out by evaluating the fluid film forces under the short bearing assumption. Using these forces the steady-state equilibrium position of the journal bearing was obtained. The fluid film forces were then used to determine the bearing dynamic coefficients (inertia effects, damping and stiffness parameters).

2. Mathematical Modeling

2.1 *Journal Bearing Set with Molten Zinc Lubricant*

The system analyzed in this work consisted of only one-half of the galvanizing process setup, taking advantage of the symmetry of the system about the middle journal plane. Under the rigid supports assumption, in a reference fixed to bearings, a *Oxyz* right-handed rectangular cartesian coordinate system was used, as shown in Fig. 2. The molten zinc separates the rotating journal (roller) from the stationary bearing, and the pressure developed in the radial clearance of the bearing supports the static load, as well as any dynamic load due to external disturbances.

Fluid viscosity and type of fluid (Newtonian or non-Newtonian) are the two major lubricant characteristics that influence the hydrodynamic properties of a journal bearing set. The viscosity of the molten zinc is dependent upon composition (i.e., percentage of the other elements such as Pb, Al, etc.) and temperature and is independent of pressure (Ref 9). Also, the molten zinc obeys the Newtonian law of viscosity (Ref 10).

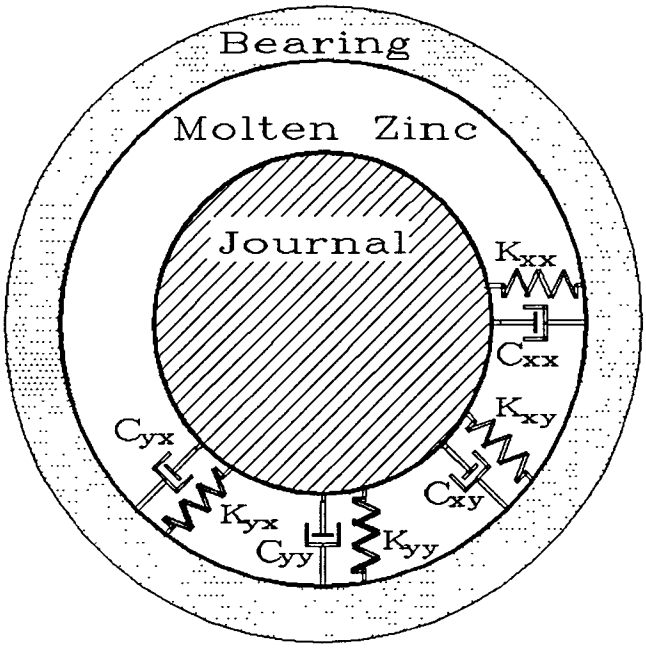

Fig. 3 Stiffness and damping properties of molten zinc (linearized model)

The mechanical properties of the molten zinc film between the journal and bearing are modeled by the standard stiffness and damper sets, as shown in Fig. 3. These stiffness and damper sets, along with the inertia of the molten zinc, determine the dynamic behavior of the rotating guide rollers. The system of spinning and orbiting roller can be modeled as a two degrees of freedom system.

The orbital motion of the journal around the steady-state equilibrium position (x_0, y_0), which is indicated by point O_J in Fig. 2, is influenced by bearing diameter D, bearing length L, radial clearance c, static load on bearing W, dynamic viscosity of molten zinc μ, and angular velocity of the journal ω. The modified Sommerfeld number σ incorporates all these parameters into a single dimensionless variable as follows:

$$\sigma = \mu\omega(RL/W)\,(R/c)^2\,(L/D)^2 \qquad \text{(Eq 1)}$$

where R is the radius of the journal. The stability of the system means that the orbital motion of the journal is well within the limits of the geometric dimensions (radial clearance, c) of the bearing. The equation of the journal motion in the cavity of the bearing can be expressed as (Ref 11):

$$\begin{bmatrix} m + C_{xx} & C_{xy} \\ C_{yx} & m + C_{yy} \end{bmatrix} \begin{Bmatrix} \ddot{x} \\ \ddot{y} \end{Bmatrix} + \begin{bmatrix} B_{xx} & B_{xy} \\ B_{yx} & B_{yy} \end{bmatrix} \begin{Bmatrix} \dot{x} \\ \dot{y} \end{Bmatrix}$$

$$+ \begin{bmatrix} K_{xx} & K_{xy} \\ K_{yx} & K_{yy} \end{bmatrix} \begin{Bmatrix} x - x_0 \\ y - y_0 \end{Bmatrix} = \begin{Bmatrix} 0 \\ 0 \end{Bmatrix} \qquad \text{(Eq 2)}$$

where m is a dimensionless mass supported by a bearing, C_{mn} is a dimensionless acceleration coefficient of lubricant film, B_{mn} is a dimensionless damping coefficient, and K_{mn} is a dimensionless stiffness coefficient. The [K], [B], and [C] matrices in Eq 2 are not symmetric. This leads to the possibility of a self-excited vibration for the orbital vibration of the roller inside the bearing clearance. This self-excited vibration of the roller can grow in amplitude up to the threshold of instability at a given roller spinning speed, ω_{cr} (proportional to the galvanizing production speed). Any increase in the production speed will cause an instability of the orbital motion of the roller. The

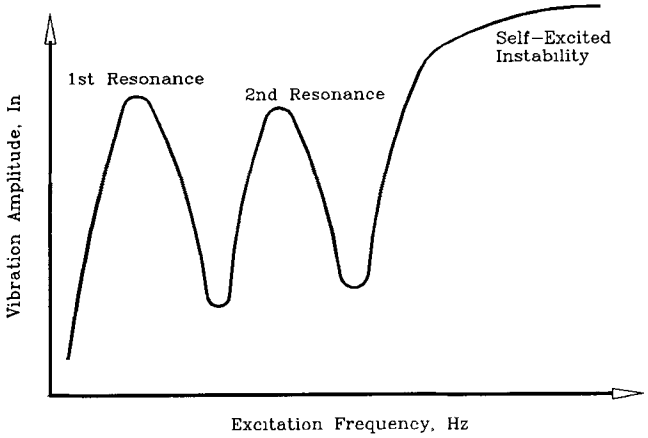

Fig. 4 Typical behavior of a vibratory system with resonance and self-excited instability characteristics

mechanism of this instability can be thought of as the impartation of energy from the spinning motion to that of the orbiting motion of the roller. Mathematically, this transfer of energy (instability mechanism) is related to the nonconservative force field stemming from the symmetric part of the [B] matrix and the skew-symmetric part of the [K] matrix (Ref 12).

The instability condition of the orbital motion of the roller is not a resonance condition. The amplitude of the orbital motion does not decrease with increase in journal angular speed, as shown in Fig. 4. A properly designed journal bearing set for a galvanizing process, with molten zinc as its lubricant, must have its ω_{cr} such that the production speed can be maintained at an acceptably high rate.

2.2 *Formulation of Mathematical Model*

For a journal bearing set under the short bearing assumption, the momentum and continuity equations in dimensionless form, respectively, are (Ref 13, 14):

$$\mathrm{Re}\frac{c}{R}\left[\frac{\partial(hw)}{\partial\tau}+\frac{1}{2}\frac{\partial(hw)}{\partial\theta}+\frac{1}{4}\frac{D}{L}\frac{\partial(hw^2)}{\partial z}\right]=-\frac{L}{D}h\frac{\partial p}{\partial z}-12G_z\frac{w}{h} \quad \text{(Eq 3)}$$

where z is the coordinate along the axial direction of the bearing, w is the velocity of the fluid in z direction, and h is the minimum film thickness.

$$\frac{\partial h}{\partial\theta}+2\frac{\partial h}{\partial\tau}+\frac{1}{2}\frac{\partial(hw)}{\partial z}=0 \quad \text{(Eq 4)}$$

where Re is the Reynolds number, τ is time, θ is angular displacement, p is pressure, G_z is the turbulence coefficient, and the dimensionless film thickness h is given by:

$$h=1-x\cos\theta-y\sin\theta \quad \text{(Eq 5)}$$

For the turbulence coefficient G_z, Capone et al. (Ref 15) have proposed an expression which considers the effects of the oil film nonlaminar flow, even when the turbulence is not developed in the whole gap:

$$G_z=1+\gamma s h\,\mathrm{Re}^{0.96} \quad \text{(Eq 6)}$$

where γ is a constant with the value of 3.47×10^{-4} and s is defined as follows:

$$s=\frac{1}{\pi}\tan^{-1}\left[\frac{2}{\pi}\frac{\mathrm{Re}_t-\mathrm{Re}_l}{\mathrm{Re}_t+\mathrm{Re}_l}\frac{\mathrm{Re}/\mathrm{Re}^*}{1-\mathrm{Re}/\mathrm{Re}^*}\right] \quad \text{(Eq 7)}$$

where

$$\mathrm{Re}_t=41.2\left[\frac{R/c}{(1-\varepsilon)^3+4/3(L/D)^2\dot{\varepsilon}^2(1-\varepsilon)}\right]^{1/2} \quad \text{(Eq 7a)}$$

$$\mathrm{Re}_l=41.2\left[\frac{R/c}{(1+\varepsilon)^3+4/3(L/D)^2\dot{\varepsilon}^2(1+\varepsilon)}\right]^{1/2} \quad \text{(Eq 7b)}$$

$$\mathrm{Re}^*=\frac{(\mathrm{Re}_t+\mathrm{Re}_l)}{2}$$

$$\varepsilon=(x^2+y^2)^{1/2}$$

$$\dot{\varepsilon}=\frac{x\dot{x}+y\dot{y}}{(x^2+y^2)^{1/2}} \quad \text{(Eq 7c)}$$

Re_t and Re_l represent the Reynolds numbers for the turbulent and laminar flow regimes, respectively.

Using continuity and momentum equations, the pressure distribution can be obtained as (Ref 1):

$$p=3\left\{\mathrm{Re}\frac{c}{R}\frac{1}{6h}\left[\frac{\partial^2h}{\partial\tau^2}+\frac{\partial^2h}{\partial\theta\partial\tau}+\frac{1}{4}\frac{\partial^2h}{\partial\theta^2}-\frac{1}{2h}\left(\frac{\partial h}{\partial\theta}+2\frac{\partial h}{\partial\tau}\right)^2\right]+\frac{G_z}{h^3}\left(\frac{\partial h}{\partial\theta}+2\frac{\partial h}{\partial\tau}\right)\right\}(4z^2-1) \quad \text{(Eq 8)}$$

Substituting Eq 6 for G_z in Eq 8 makes Eq 8 valid for any value of the Reynolds number (Ref 11).

The unsteady fluid film force components f_x and f_y can be obtained by integrating the pressure distribution, as given by Eq 8, in the intervals $\beta\le\theta\le\alpha^*$ and $-1/2\le z\le 1/2$:

$$\begin{Bmatrix}f_x\\f_y\end{Bmatrix}=-\int_{-1/2}^{1/2}\int_{\alpha^*}^{\beta}p\begin{Bmatrix}\cos\theta\\\sin\theta\end{Bmatrix}d\theta dz \quad \text{(Eq 9)}$$

2.3 *Evaluation of Dynamic Coefficients*

To evaluate the integrals in Eq 9, α^* is replaced with $\alpha=\beta-\pi$, where β is the value of θ for which $p=0$ and $\partial p/\partial\theta<0$. By doing so, it is possible for the integrals in Eq 9 to be replaced with the derivatives of opposite functions (Ref 11).

Evaluating the integrals with the above substitution, the fluid force components f_x and f_y are obtained as shown in Appendix A, Eq A1.

The bearing dynamic coefficients now can be obtained from the derivatives of the above fluid force components. An infinitesimal variation in α results in an infinitesimal variation of a high order in the components f_x and f_y of the fluid film force. Also, it is assumed that the flow regime does not vary around the steady state and coincides with the regime corresponding to the steady state itself. Hence, the dynamic coefficients can be evaluated by taking α and s as constants. The bearing dynamic coefficients (stiffness, damping, and inertia coefficients) can be determined as shown in Appendix A, Eq A8 to A17.

With the bearing dynamic coefficients determined, the analysis of the stability of the system can be carried out by evaluating its eigenvalues, λ. The motion of the journal about the steady-state equilibrium position is described by Eq 2. Assuming a solution of the form

$$\begin{Bmatrix} x - x_0 \\ y - y_0 \end{Bmatrix} = \begin{Bmatrix} X \\ Y \end{Bmatrix} e^{\lambda \tau} \quad \text{(Eq 10)}$$

we obtain:

$$\begin{bmatrix} (m + c_{xx})\lambda^2 + B_{xx}\lambda + K_{xx} & C_{xy}\lambda^2 + B_{xy}\lambda + K_{xy} \\ C_{yx}\lambda^2 + B_{yx}\lambda + K_{yx} & (m + c_{yy})\lambda^2 + B_{yy}\lambda + K_{yy} \end{bmatrix} \begin{Bmatrix} X \\ Y \end{Bmatrix} = \begin{Bmatrix} 0 \\ 0 \end{Bmatrix} \quad \text{(Eq 11)}$$

Equating to zero the determinant of the above linear homogeneous system, the characteristic equation of the system is obtained as follows:

$$\begin{aligned} &(-c_{yx}c_{xy} + mc_{yy} + mc_{xx} + c_{xx}c_{yy} + m^2)\lambda^4 \\ &+ (-c_{yx}B_{xy} + B_{xx}c_{yy} + c_{xx}B_{yy} + mB_{yy} - B_{yx}c_{xy} + mB_{xx})\lambda^3 \\ &+ (-c_{yx}K_{xy} + B_{xx}B_{yy} - B_{yx}B_{xy} + c_{xx}K_{yy} - K_{yx}c_{xy} + mK_{yy} \\ &+ K_{xx}c_{yy} + mK_{xx})\lambda^2 + (B_{xx}K_{yy} + K_{xx}B_{yy} - K_{yx}B_{xy} - B_{yx}K_{xy})\lambda \\ &+ K_{xx}K_{yy} - K_{xy}K_{yx} = 0 \end{aligned} \quad \text{(Eq 12)}$$

The stability of the system can be analyzed using the eigenvalues, λ, determined from the above characteristic equation.

3. Parametric Study of the Model

3.1 *Journal Bearing Parameters*

The theory described in the preceding sections is implemented here for two test cases. Table 1 gives the bearing geometry and the journal angular velocity for which the test cases were evaluated. The journal angular velocity given in Table 1 (44.401 rad/s) is equivalent to the galvanizing production rate of 2.54 m/s (500 ft/min).

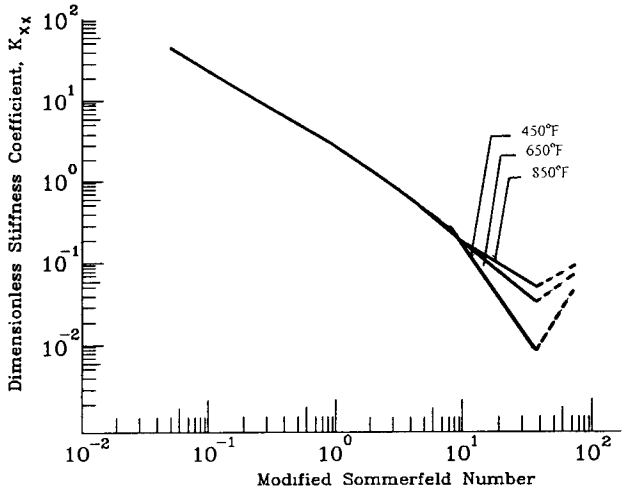

Fig. 5 Dimensionless stiffness coefficients versus modified Sommerfeld number for zinc purity = 86% (solid line, positive; dashed line, negative)

These test cases were carried out for typical galvanizing process operating temperatures of 450, 650, and 850 °F. For each of these temperatures the test cases were carried out for 86 and 100% of purity of zinc. Table 2 gives the viscosity values of the molten zinc for the above temperatures and purities, and Table 3 gives the values of molten zinc density at the above temperatures (Ref 8).

Table 1 Journal bearing test case parameters

L, m	*D*, m	*c*, m	ω, rad/s	*m*/2, kg
0.25	0.25	0.000051	44.401	317.53

Table 2 Viscosity values of molten zinc

Temperature, °F	Viscosity for 86% zinc, Pa · s	Viscosity for 100% zinc, Pa · s
450	0.00176	0.00285
650	0.0013	0.00208
850	0.00107	0.00165

Table 3 Density values of molten zinc

Temperature, °F	Density, kg/m^3
450	6600
650	6400
850	6200

Table 4 Reynolds numbers (Re) for test cases

Temperature, °F	Re for 86% zinc	Re for 100% zinc
450	0.00176	0.00285
650	0.0013	0.00208
850	0.00107	0.00165

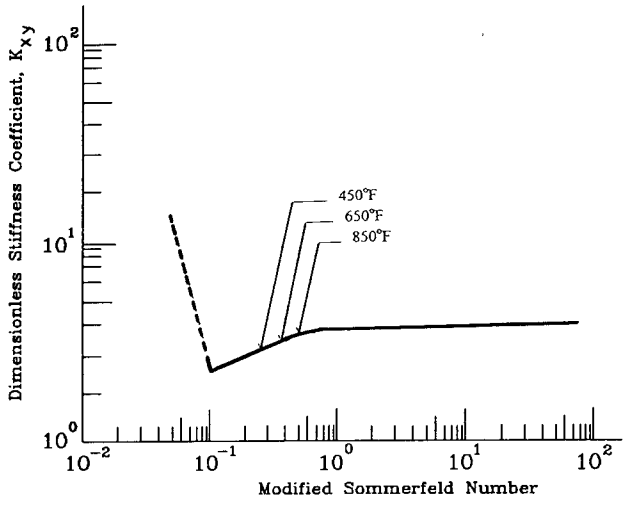

Fig. 6 Dimensionless stiffness coefficients versus modified Sommerfeld number for zinc purity = 86% (solid line, positive; dashed line, negative)

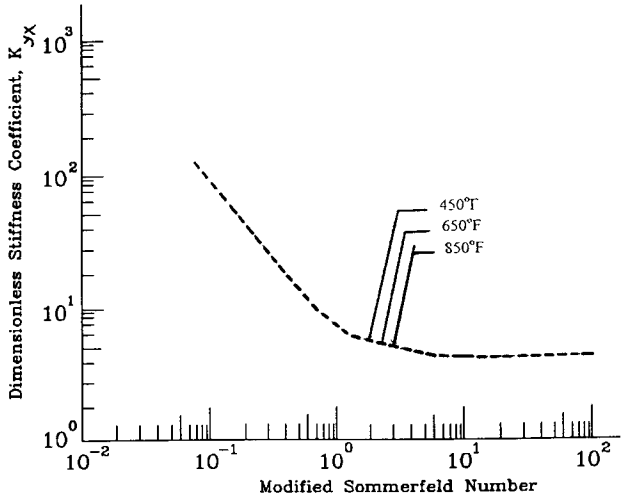

Fig. 7 Dimensionless stiffness coefficients versus modified Sommerfeld number for zinc purity = 86% (solid line, positive; dashed line, negative)

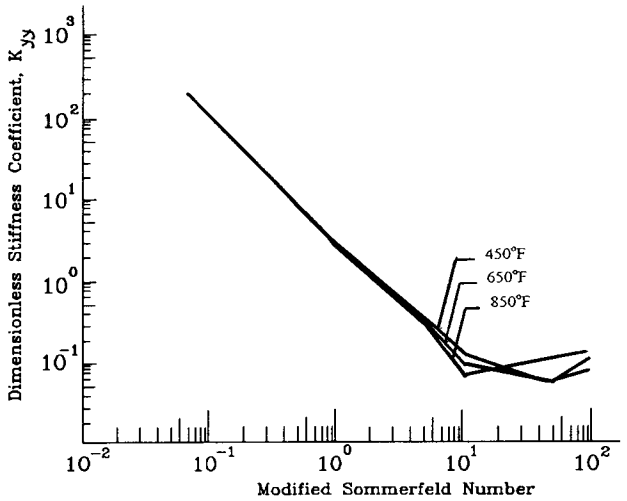

Fig. 8 Dimensionless stiffness coefficients versus modified Sommerfeld number for zinc purity = 86% (solid line, positive; dashed line, negative)

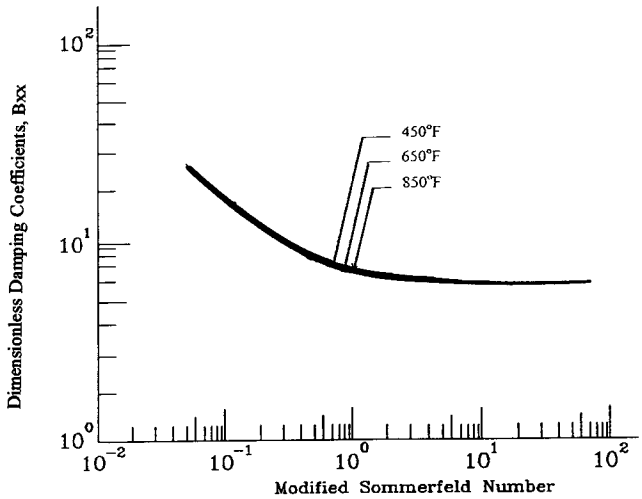

Fig. 9 Dimensionless damping coefficients versus modified Sommerfeld number for zinc purity = 86% (solid line, positive; dashed line, negative)

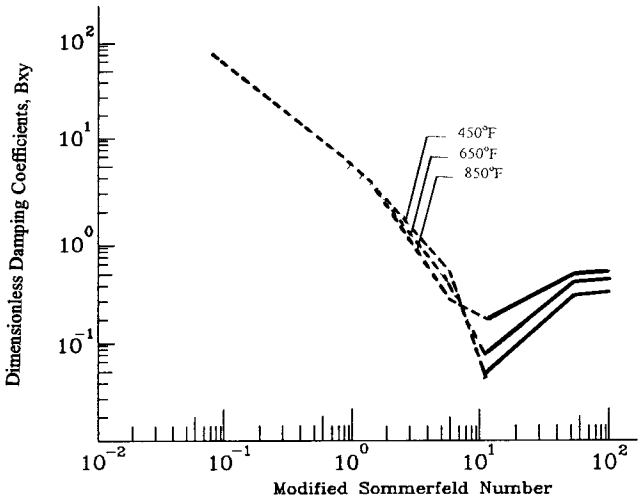

Fig. 10 Dimensionless damping coefficients versus modified Sommerfeld number for zinc purity = 86% (solid line, positive; dashed line, negative)

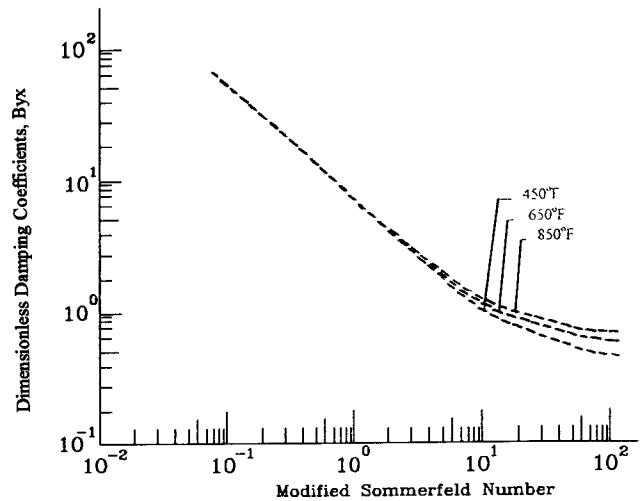

Fig. 11 Dimensionless damping coefficients versus modified Sommerfeld number for zinc purity = 86% (solid line, positive; dashed line, negative)

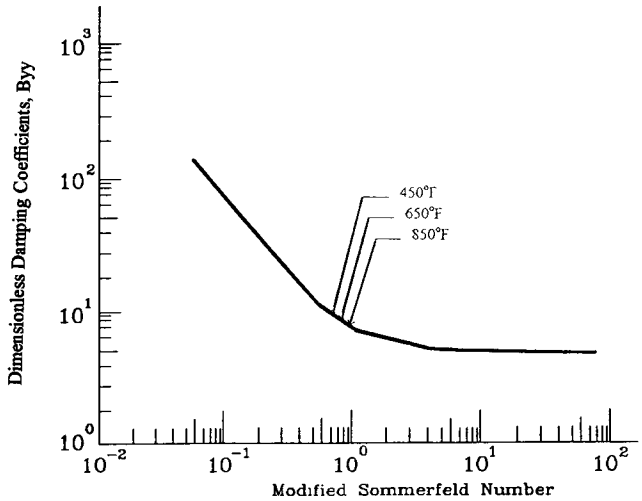

Fig. 12 Dimensionless damping coefficients versus modified Sommerfeld number for zinc purity = 86% (solid line, positive; dashed line, negative)

Table 5 Bearing dynamic coefficients for temperature = 450 °F and zinc purity = 86 %

σ	K_{xx}	K_{xy}	K_{yx}	K_{yy}	B_{xx}	B_{xy}	B_{yx}	B_{yy}	C_{xx}	C_{xy}	C_{yx}	C_{yy}
0.05	37.63602317	−12.32595979	−104.0520664	167.044291	24.30579902	−38.65004808	−39.38355262	159.5271544	0.21323906	−0.020914491	−0.020914491	0.520265498
0.1	19.84968483	−2.052712575	−45.75763053	56.99377965	16.40598406	−20.16099976	−20.79900449	71.30826357	0.210000007	−0.031027316	−0.031027316	0.428004718
0.5	4.595629318	2.988202991	−8.070613056	4.488077357	8.288452964	−4.453669865	−4.950378899	13.8689815	0.216745797	−0.03279962	−0.03279962	0.279963234
1	2.387406917	3.167123417	−4.828231412	1.601941545	7.098368909	−2.221770523	−2.69130571	8.842351456	0.222020227	−0.023698127	−0.023698127	0.24751496
5	0.450883714	3.159363511	−3.257605799	0.202397654	6.362358651	−0.280470348	−0.734594809	6.437205003	0.226395723	−0.006012008	−0.006012008	0.227728736
10	0.19773663	3.150722292	−3.181351811	0.071140515	6.31474473	−0.027509769	−0.481099271	6.331357587	0.226638548	−0.003043617	−0.003043617	0.22695095
50	−0.005739588	3.143433142	−3.146501582	−0.031252871	6.288126445	0.175820651	−0.277672221	6.288070545	0.22674677	−0.00061377	−0.00061377	0.226746101
100	−0.031202252	3.142516011	−3.143850604	−0.043984031	6.2855571	0.201322948	−0.252179283	6.285339009	0.226740654	−0.00031091	−0.00031091	0.226761571

Table 6 Bearing dynamic coefficients for temperature = 450 °F and zinc purity = 100 %

σ	K_{xx}	K_{xy}	K_{yx}	K_{yy}	B_{xx}	B_{xy}	B_{yx}	B_{yy}	C_{xx}	C_{xy}	C_{yx}	C_{yy}
0.05	37.48373614	−12.19639939	−103.9549815	167.6103454	24.09802799	−38.62450881	−39.07775299	159.5553801	0.131680312	−0.012624172	−0.012624172	0.321563844
0.1	19.75539647	−2.01621849	−45.7514653	57.37326417	16.22519961	−20.17683005	−20.5712068	71.34802204	0.129639707	−0.018834443	−0.018834443	0.264737037
0.5	4.600411431	2.936310551	−8.07104596	4.582637194	8.156422595	−4.534319007	−4.841604769	13.86264538	0.133692612	−0.020150961	−0.020150961	0.173593153
1	2.409965562	3.119464738	−4.786513151	1.638986718	6.993627702	−2.311831941	−2.6021624	8.798930877	0.137018871	−0.014683189	−0.014683189	0.153311592
5	0.47307581	3.145905151	−3.231132734	0.223932192	6.332170372	−0.367844327	−0.648357519	6.412262948	0.139823493	−0.003727178	−0.003727178	0.1406897
10	0.219493381	3.14397007	−3.167423172	0.0928415	6.299521603	−0.11439203	−0.394540266	6.318274457	0.13996949	−0.001883765	−0.001883765	0.140178747
50	0.015924809	3.142092462	−3.143665692	−0.009546926	6.28510643	0.089104106	−0.190955348	6.285400122	0.140027029	−0.00037746	−0.00037746	0.140032425
100	−0.009532311	3.14184626	−3.14243217	−0.022288195	6.284051125	0.11460162	−0.165459776	6.284000675	0.140018937	−0.00019197	−0.00019197	0.140042463

Table 7 Eigenvalues for temperature = 850 °F and zinc purity = 86 %, excluding the acceleration coefficients

σ	Eigenvalue 1	Eigenvalue 2	Eigenvalue 3	Eigenvalue 4
0.05	−1.1739 + 0.8449 j	−1.1739 − 0.8449 j	−3918.2681	−47,490.0209
0.1	−0.9165 + 0.6714 j	−0.9165 − 0.6714 j	−2729.9180	−21,816.9862
0.5	−0.4180 + 0.53021 j	−0.4180 − 0.53021 j	−1639.3483	−4, 646.8470
1	−0.2562 + 0.5084 j	−0.2562 − 0.5084 j	−1592.7154	−3, 010.4729
5	−0.0712 + 0.5036 j	−0.0712 − 0.5036 j	−1729.8523	−1, 933.6015
10	−0.0432 + 0.5018 j	−0.0432 − 0.5018 j	−1790.1261 + 66.9007 j	−1790.1261 − 66.9007 j
50	−0.0198 + 0.4997 j	−0.0198 − 0.4997 j	−1761.5504 + 96.3305 j	−1761.5504 − 96.3305 j
100	−0.0168 + 0.4992 j	−0.0168 − 0.4992 j	−1758.3584 + 97.1181 j	−1758.3584 − 97.1181 j

Table 8 Eigenvalues for temperature = 850 °F, and zinc purity = 86 %, and Reynolds number = 4920

σ	Eigenvalue 1	Eigenvalue 2	Eigenvalue 3	Eigenvalue 4
0.05	−1.1617 + 0.7296 j	−1.1617 − 0.7296 j	−13.7271	−73.2811
0.1	−0.8438 + 0.4352 j	−0.8438 − 0.4352 j	−11.3824	−39.9217
0.5	−0.6468 + 0.4285 j	−0.6468 − 0.4285 j	−3.7564	−11.3158
1	−0.3445 + 0.4732 j	−0.3445 − 0.4732 j	−4.2443	−7.7010
5	−0.0636 + 0.4906 j	−0.0636 − 0.4906 j	−5.7082 + 0.3709 j	−5.7082 − 0.3709 j
10	−0.0307 + 0.4952 j	−0.0307 − 0.4952 j	−5.8002 + 0.4663 j	−5.8002 − 0.4663 j
50	−0.0057 + 0.4990 j	−0.0057 − 0.4990 j	−5.8921 + 0.4898 j	−5.8921 − 0.4898 j
100	−0.0026 + 0.4995 j	−0.0026 − 0.4995 j	−5.9047 + 0.4901 j	−5.9047 − 0.4901 j

With all of the above data, computer runs were made for each of the test cases for modified Sommerfeld number values of 0.05, 0.1, 0.5, 1, 5, 10, 50, and 100, which correspond to varying loads on the bearing.

In addition to the above cases, the eigenvalues for zinc purity of 86% at 850 °F were evaluated without considering the acceleration coefficients. These eigenvalues were compared with the eigenvalues obtained by considering the acceleration coefficients for the same case, to determine the influence of the oil film inertia. The numerical values obtained for the above runs are given in the results section.

3.2 *Study of the Influence of Flow Regime*

The type of flow regime in the bearing cavity is determined by the Reynolds number, which is defined as:

$$Re = \rho\omega Rc/\mu \qquad \text{(Eq 13)}$$

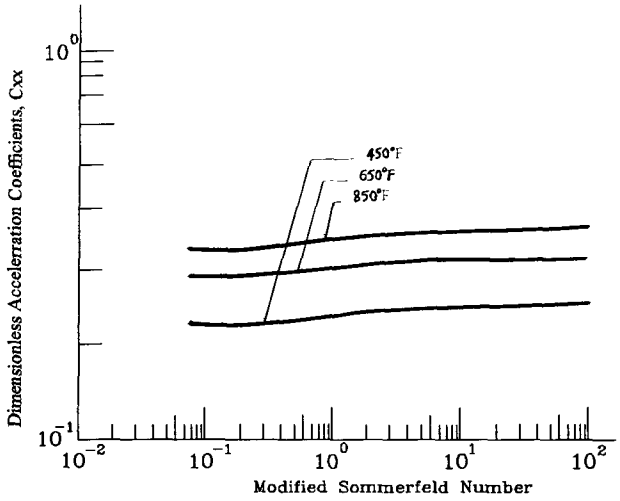

Fig. 13 Dimensionless acceleration coefficients versus modified Sommerfeld number for zinc purity = 86% (solid line, positive; dashed line, negative)

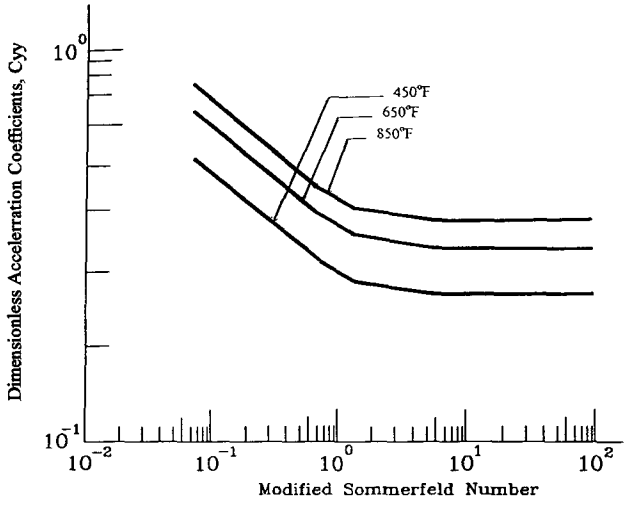

Fig. 15 Dimensionless acceleration coefficients versus modified Sommerfeld number for zinc purity = 86% (solid line, positive; dashed line, negative)

where ρ is the molten zinc density. For the journal bearing described here, the critical Reynolds number Re_c is given as (Ref 8):

$$Re_c = \frac{41.1}{\sqrt{(2c/D)}} \qquad \text{(Eq 14)}$$

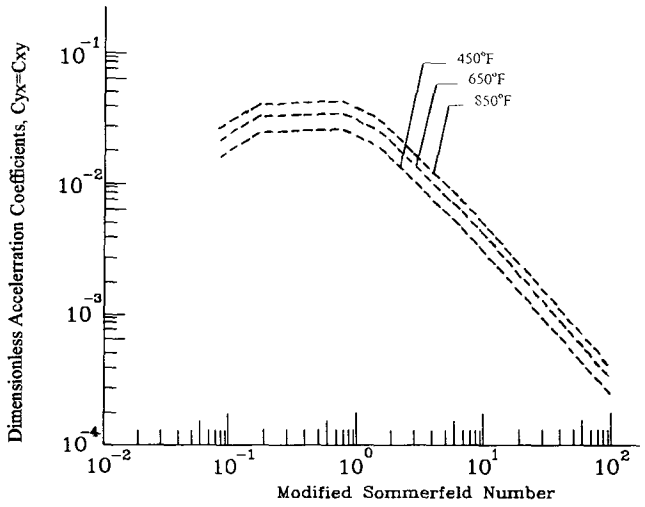

Fig. 14 Dimensionless acceleration coefficients versus modified Sommerfeld number for zinc purity = 86% (solid line, positive; dashed line, negative)

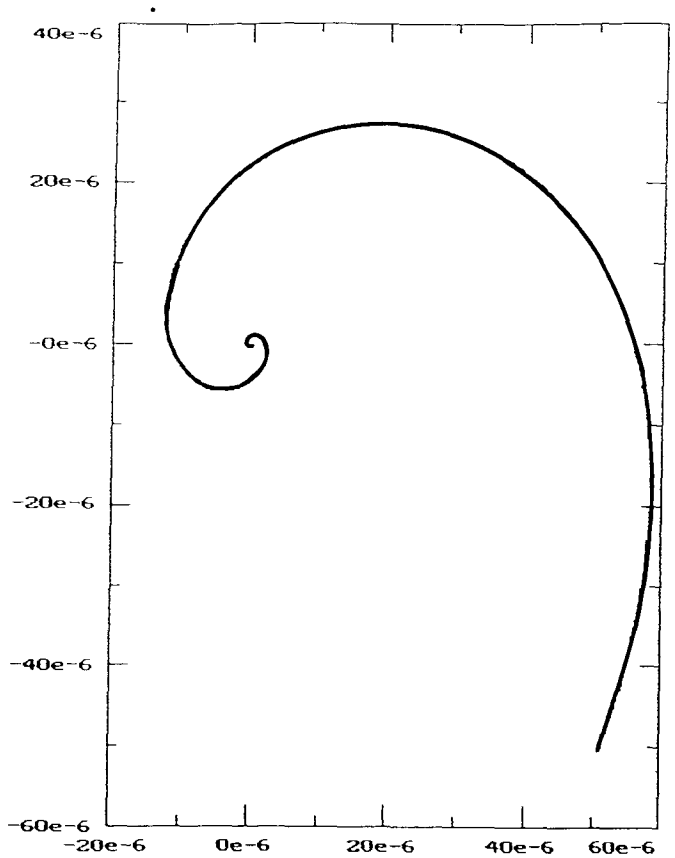

Fig. 16 Time response curve for zinc purity = 86%, temperature = 450 °F, and modified Sommerfeld number = 1

For the parameters given in Table 1, $Re_c = 2034.8$. The Reynolds number for the test cases are given in Table 4.

All of the test cases had Reynolds numbers less than Re_c. Hence, the flow regime for all of the above test cases was laminar. To determine the effects of a turbulent flow regime, a computer run was made with journal angular velocity $\omega = 133.203$ rad/s, for zinc purity of 86% at 850 °F. For this case Re = 4920.4191, which is above the Re_c number. Therefore this case had a turbulent flow regime. The numerical values obtained for the above runs are given in the results section.

4. Results

4.1 *Dynamic Coefficients, Eigenvalues, and Time Response Curves*

Using the parameters given in the preceding sections, dynamic coefficients, eigenvalues, and the time response of the system were evaluated. Tables 5 and 6 give the bearing dynamic coefficients for 86 and 100% zinc alloys at 450 °F. Bearing dynamic coefficients for other zinc alloys at 650 and 850 °F are given in Appendix B in Tables B1 to B4. The bearing stiffness properties with 86% molten zinc as the lubricant are each plotted as a function of the modified Sommerfeld number σ for three different temperatures in Fig. 5 to 8. Figures 9 to 12 and Fig. 13 to 15 depict the bearing damping and inertia properties, respectively, for 86% molten zinc alloy as the bearing lubricant. The bearing dynamic coefficients (stiffness, damping, and inertia effects) for 100% molten zinc are plotted versus the modified Sommerfeld number in Appendix C. These graphs indicate that K_{xy}, K_{yx}, B_{xx}, and B_{yy} values do not vary with temperature. Even K_{xx}, K_{yy}, B_{xy}, and B_{yx} values undergo small variation with temperature only at higher values of σ. Values for the parameters C_{xx}, C_{xy}, C_{yx}, and B_{yy} increase with increasing temperature. The purity of zinc does not have any effect on any dynamic coefficients.

The eigenvalues of the system calculated from the dynamic coefficients are given in Appendix D in Tables D1 to D6. It can be seen from these tables that neither temperature nor zinc purity has any noticeable effects on the eigenvalues or, hence, on the stability of the system for the assumed operating conditions.

The orbital motions of the journal (roller) inside the bearing are given in Fig. 16 through 18. As expected, the trajectories of the cases for which the eigenvalues have small negative real parts show more loops. The trajectory of the case that has the largest negative real parts in its eigenvalues converges rapidly to its equilibrium position.

4.2 *Effects of Lubricant Film (Molten Zinc) Inertia and Flow Regime*

To study the influence of lubricant film inertia, eigenvalues were calculated for the test case of zinc purity of 86% at 850 °F without considering the acceleration coefficients. These eigenvalues are given in Table 7. The eigenvalues for the same case, taking into consideration the acceleration coefficients, are given in Appendix D in Table D2. Comparing the values from the two tables, it can be seen that the effect of the oil film inertia is to reduce value of the real part of the eigenvalues. In other words, the results of analysis of a stable bearing approaches the threshold of instability as the inertia effects of the molten zinc

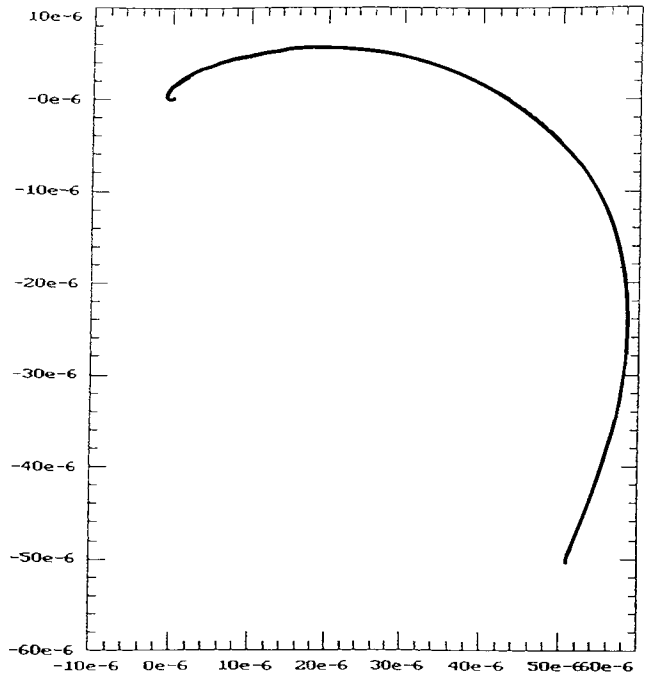

Fig. 17 Time response curve for zinc purity = 100%, temperature = 650 °F, and modified Sommerfeld number = 0.05

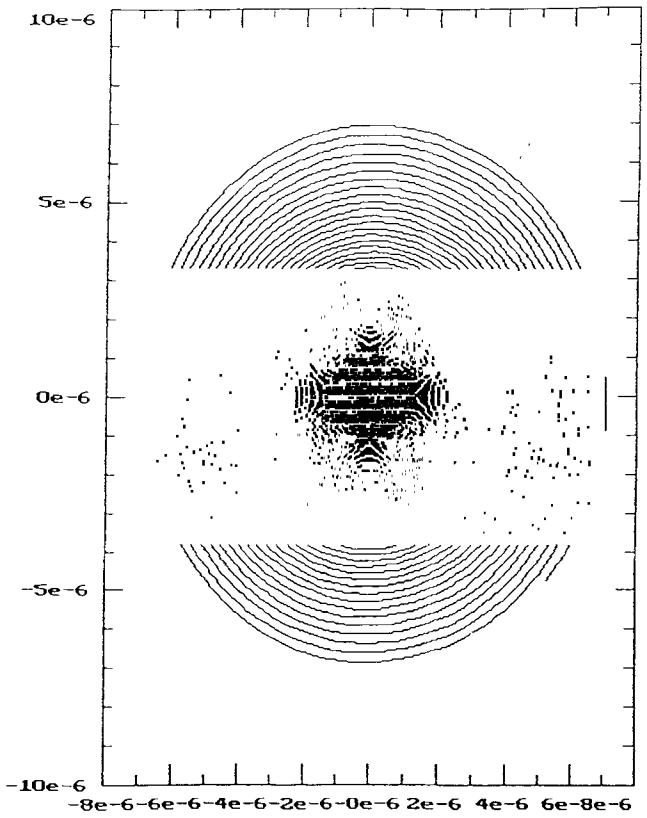

Fig. 18 Time response curve for zinc purity = 100%, temperature = 850 °F, and modified Sommerfeld number = 100

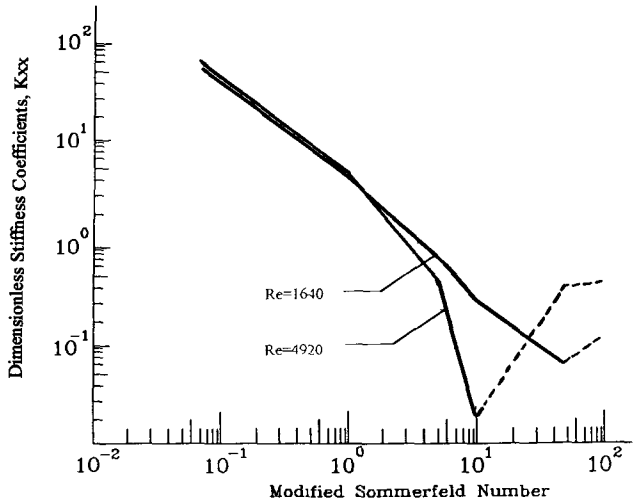

Fig. 19 Dimensionless stiffness coefficients versus modified Sommerfeld number for temperature = 850 °F and zinc purity = 86% (solid line, positive; dashed line, negative)

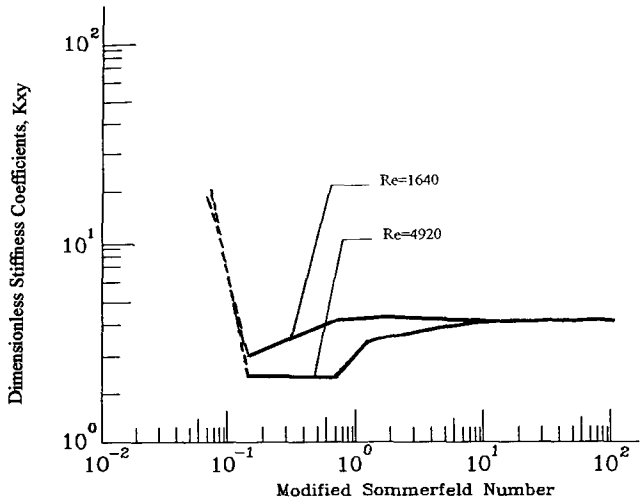

Fig. 20 Dimensionless stiffness coefficients versus modified Sommerfeld number for temperature = 850 °F and zinc purity = 86% (solid line, positive; dashed line, negative)

are included in the mathematical model of the system. This means that for design purposes, the inclusion of inertia coefficients provides a more conservative result, guarding against bearing instability.

To evaluate the effects of flow regime, a computer test run was made for the case of zinc purity of 86% at 850 °F with Re = 4920. This Reynolds number corresponds to journal angular velocity $\omega = 133.203$ rad/s, and it also indicates that the flow regime in the bearing gap is turbulent. The dynamic coefficients evaluated for this case are plotted against modified Sommerfeld number in Fig. 19 and 20 and also in Appendix E in Fig. E1 to E9. These figures also contain the dynamic coefficients given in Appendix B, Table B3, for the same case, but with Re = 1640.

The eigenvalues for Re = 1640 are given in Appendix D, Table D2. Comparing these eigenvalues with those in Table 8, it can be seen that the eigenvalues of the turbulent regime have smaller negative real parts. Therefore, as expected, the effect of the turbulent regime is to reduce the stability of the system.

5. Conclusions

This paper has attempted to improve the theoretical predictions of journal bearing behavior by taking into account the effects of turbulence and fluid inertia. A major assumption made in this work is that no chemical reactions take place between the molten zinc and journal bearing material(s). Any chemical reaction may affect the mechanical properties of the molten zinc within the bearing radial clearance and hence influence the bearing performance.

References

1. P.G. Morton, Dynamic Characteristics of Bearings Measurements under Operating Conditions, *GEC J. Sci. Technol.*, Vol 42, 1975, p 37-47
2. J.W. Lund, E.B. Arwas, H.S. Chen, C.W. Ng, C.H.T. Pan, and B. Sternlich, "Rotor Bearings Dynamics Technology, Part 3," Technical Report AFAPL TR-65-45, Wright-Patterson Air Force Base, OH, 1965
3. D.W. Parkins, Theoretical and Experimental Determination of the Dynamic Characteristics of Hydrodynamic Journal Bearings, *J. Lub. Technol.*, Vol 101, April 1979, p 129-139
4. P.D. Williams and G.R. Symmons, Analysis of Hydrodynamic Slider Thrust Bearings Lubricated with Non-Newtonian Fluids, *Wear*, Vol 117, 1987, p 91-102
5. B. Najji, B. Bou-Said, and D. Berthe, New Formulation for Lubrication with Non-Newtonian Fluids, *ASME Trans., J. Tribol.*, Jan 1989, p 29-34
6. J.F. Hutton, K.P. Jackson, and B.P. Williamson, The Effects of Lubricant Rheology on the Performance of Journal Bearings, *ASLE Trans.*, Vol 29 (No. 1), 1984, p 52-60
7. R.H. Buckholz, On the Role of a Non-Newtonian Fluid in Short Bearing Theory, *ASME Trans., J. Tribol.*, Vol 107, Jan 1985, p 69-74
8. M. Rashidi, Modeling and Analysis of Journal Bearings Lubricated with Molten Zinc for Galvanizing Process, *J. Mater. Eng. Perform.*, Vol 1 (No. 3), June 1992, p 324-331
9. T.P. Yao and V. Kondic, The Viscosity of Molten Tin, Lead, Zinc, Aluminium, and Some of Their Alloys, *J. Inst. Metals*, Vol 81, 1952-1953, p 17-24
10. J. Szekely, *Fluid Flow Phenomena in Metals Processing*, Academic Press, 1977
11. G. Capone, M. Russo, and R. Russo, Inertia and Turbulence Effects on Dynamic Characteristics and Stability of Rotor-Bearings Systems, *ASME Trans.*, Vol 113, Jan 1991, p 58-64
12. M.L. Adams and J. Padovan, Insights into Linearized Rotor Dynamics, *J. Sound Vibrations*, Vol 76 (No. 1), 1981, p 129-142
13. V.N. Constantinescu, On the Influence of Inertia Forces in Turbulent and Laminar Self-Acting Films, *J. Lub. Technol.*, Vol 92, 1970, p 473-481
14. A.Z. Szeri, *Tribology*, McGraw-Hill, 1980
15. G. Capone, M. Russo, and R. Russo, Dynamic Characteristics and Stability of a Journal Bearing in a Non-Laminar Regime, *Tribol. Internat.*, Vol 20 (No. 5), 1987, p 255-260